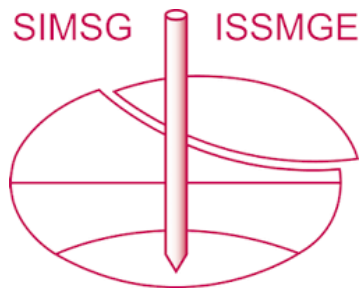


# INTERNATIONAL SOCIETY FOR SOIL MECHANICS AND GEOTECHNICAL ENGINEERING



*This paper was downloaded from the Online Library of the International Society for Soil Mechanics and Geotechnical Engineering (ISSMGE). The library is available here:*

<https://www.issmge.org/publications/online-library>

*This is an open-access database that archives thousands of papers published under the Auspices of the ISSMGE and maintained by the Innovation and Development Committee of ISSMGE.*

*The paper was published in the Proceedings of the 8<sup>th</sup> International Symposium on Deformation Characteristics of Geomaterials (IS-PORTO 2023) and was edited by António Viana da Fonseca and Cristiana Ferreira. The symposium was held from the 3<sup>rd</sup> to the 6<sup>th</sup> of September 2023 in Porto, Portugal.*

# The short DMTA dissipation test

Emőke Imre<sup>1\*</sup>, Diego Marchetti<sup>2</sup>, Miklós Juhász<sup>3</sup>, Lachlan Bates<sup>4</sup>, Stephen Fityus<sup>5</sup> and Vijay P. Singh<sup>6</sup>

<sup>1</sup>Óbuda University, Hungary

<sup>2</sup>Studio Prof. Marchetti Italy <sup>3</sup>Debrecen University, Hungary

<sup>4</sup>University of Newcastle, Newcastle, Australia

<sup>5</sup>Douglas Partners, Newcastle, Australia

<sup>6</sup>Texas A&M University, USA.

\* Corresponding author: imre.emoke@uni-obuda.hu

## ABSTRACT

The CPT is used either in a continuous advance mode or in a rheological testing mode. Both periods are present in the short local side friction and in the short cone resistance dissipation tests made in the technical breaks of continuous penetration of the old CPT S832 equipment. The pause is a few second long. A statistical study previously made revealed that the local side resistance increased in sand and decreased in NC plastic soils with time in the first seconds after the stop of the steady penetration, the decrease was sometimes larger than 50%. The rate of stress variation was depending on the permeability and thus on the soil type. In this research, a similar, new test is considered. Before taking the standard *A-reading* in a DMT, a short dissipation can be measured in a generally 15 s long time period, with the Medusa DAS, being able to sample an *A-reading* in every 20 millisecond. A series of them made at the Araquari test sites are statistically analysed here. The results are similar to the ones related to the short local side friction dissipation tests which is explained by the different residual stress state in sands and in NC clays, and by the different permeability of sands and NC clays.

**Keywords:** coupled consolidation; point-symmetric; pore water dissipation; total stress dissipation.

## 1. Introduction

Whilst a range of “long” in situ dissipation tests are possible (such as those listed in Table 1) they are generally not evaluated and used, except the CPTu  $u_2$  pore water pressure and the DMTA dissipation test (Totani at al, 1998). These are evaluated on the basis of 50% long data series. Concerning the shorter versions, only the S832 shaft and tip resistance dissipation tests have an empirical evaluation mode. The aim of the paper is to suggest a similar, empirical evaluation mode for the short DMTA dissipation test.

### 1.1 S832 CPT short dissipation test

#### 1.1.1 General

Initially, the first short dissipation tests were made after deliberately pausing the steady penetration of the S832 CPT equipment due to technical reasons. The time variation of the analogue local side friction and cone resistance were recorded for a duration of seconds.

The general geometry of the S832 CPT penetrometer cone tip is in accordance with the recommended limits (defined in ICSMFE 1977). The friction sleeve is located immediately above the tip with surface area of  $A=350 \text{ cm}^2$  which is slightly larger than value  $A=250 \text{ cm}^2$  generally used by other systems). The *logging test* is facilitated by the periodic pushing of the S832 cone (the rod of the penetrometer is released after every one meter of stroke, which is unlike most systems where it is pushed continuously). The rate of penetration may vary between 0.0065 to 3.75 m/min.

**Table 1.** Types of dissipation tests made with in situ equipment

| Variable                | Test notation            | Test name                                                         |
|-------------------------|--------------------------|-------------------------------------------------------------------|
| Pore water pressure     | CPTu $u_2$ $u_3$ etc.    | pore water pressure dissipation                                   |
| Total stress            | PSL*<br>DMTA<br>DMTC     | piezo-lateral stress cell<br>DMTA-dissipation<br>DMTC-dissipation |
| Shaft or tip resistance | CPT- $f_s$<br>CPT- $q_c$ | $f_s$ dissipation<br>$q_c$ dissipation                            |

\* also pore water pressure

The short dissipation test was performed with the S832 equipment in every 50 cm, when the steady penetration was stopped, the rod was re-clamped, but the local side friction  $f_s$  and the cone resistance  $q_c$  continued to be measured. The 50 cm frequency may give sufficient information on the layer boundaries since the affected zone extends several tens of diameters away.

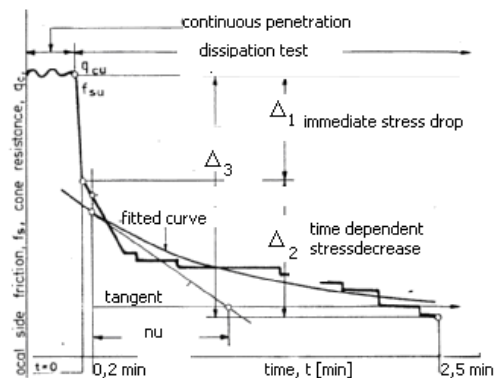


**Figure 1.** Measured S832 CPT short  $f_s$  and  $q_c$  dissipation tests, analogue outputs with parameters. (using Imre 1995).

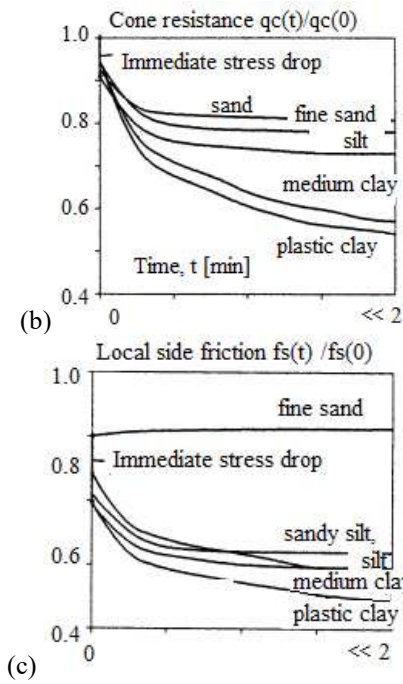


**Figure 2.** (a) The mean  $q_c$ -time relations; (b) The mean  $f_s$ -time relation (Imre et al. 2010). Note that time scale is approximate.

### 1.1.2 Empirical, statistical and qualitative evaluation

The analogue S832 CPT short dissipation output is saw-tooth-like, as shown in Fig. 1. Note that for this early CPT equipment, the time scale was not available, is approximate.

The time variation of the short dissipation showed an immediate stress drop and a time dependent stress drop (Fig. 1). The records were digitalized using uniform time cells and characterized by some parameters. The delta parameter of the time dependent stress drop for the local side friction  $\Delta f_{s2}$  (Fig. 1) is given by:

$$\Delta f_{s2} = f_s(t_i) - f_s(t_i + t_1); \quad (1)$$

where  $t_i$  is the time of the immediate stress drop at the breaking point of the graph, and  $t_1$  is a reference time.

An additional rate parameter  $\nu$  was defined by fitting the relaxation equation of the Poynting-Thomson model on the stress  $\sigma$  measured during the time dependent period (Fig. 1). The empirical relaxation equation of the Poynting-Thomson model:

$$\sigma(t) = \sigma_\infty + (\sigma_0 - \sigma_\infty) e^{-\frac{t}{\nu}} \quad (2)$$

Concerning the statistical evaluation, a total of 135 rheological type cone penetration test records were selected from the data bank of the Geodesical and Geotechnical Institute (FTV). The parameters shown in Fig. 1 were computed for the selected short  $f_s$  and  $q_c$  dissipation type CPT measurements.

The related test sites were characterized as follows (Imre 1995). The Debrecen site is in the eastern part of the city of Debrecen, Hungary, where Pleistocene wind-transported sand is found below the groundwater level, between average depths of 2.5 m and 10.0 m below the surface. In the Szeged test site the geological structure consists of the following sequence of layers: topsoil;

Pleistocene infusion loess ("Mo" is a soil with plasticity index values  $I_p$  less than 10 %); yellow lacustrine clay; and bluish-grey fresh-water silt-clay, the soils are NC except a crust. Some soil samples were taken from ten boreholes for laboratory testing.

From the dissipation tests related to the same layers, with similar plasticity index  $I_p$ , mean dissipation test records were determined (Fig. 2, Imre et al. 2010). According to then results, the shaft resistance decreased or increased during the time dependent dissipation period in the first minute for plastic or granular soils, respectively. The delta parameter increased with soil plasticity (and decreasing permeability).

Factor analysis was made with the in situ and lab test data. Results indicated strong correlations among the identified parameters, permeability and plasticity index  $I_p$ , except at layer boundaries or in the case of the crust layers with secondary structure (where the permeability was larger than expected from  $I_p$ ).

Concerning the qualitative evaluation of these results, a parameter analysis was made with the suggested joined model (ie., a coupled consolidation model with time dependent constitutive equation (Imre et al. 2010) and the empirical parameters were simulated. The time variation of the radial effective stress was a decrease or increase during the first minute for small and large permeability soils, respectively, in accordance with the measured data.

The simulated empirical parameters indicated the same dependence on the permeability and the plasticity index  $I_p$  as the real empirical parameters. The permeability depends on soil plasticity in the NC intact layers. The empirical parameters can be used for approximate soil identification.

### 1.2 Short DMTA dissipation test procedure

DMTA dissipation test means that the  $A$ -pressure is measured before the standard  $A$ -reading. It can be noted that the DMT  $A$ -pressure is considered as a radial total stress, while it is actually a fluid pressure as follows (Monaco, 2021).

The concept of  $A$ -reading is summarized here. The electric contact between the sensing disc and the membrane of the blade is provided by the steel spring and steel cylinder, they increase the hydraulic pressure to the membrane.

When the internal oil pressure equals the external soil pressure, the membrane lifts-off from its seat and starts to expand laterally. When the membrane is expanded of 0.05 mm at its centre, the electric contact between the membrane and the sensing disc is deactivated and the pressure is recorded as the  $A$ -reading.

The pressurization rate is regulated so that the so called standard  $A$ -reading is obtained in approximately 15 s after reaching the test depth (i.e. start of pressurization), with  $\pm 5$  s tolerance as with the traditional pneumatic dilatometer (ASTM D6635-15, ISO 22476-11:2017(E)).

The B reading is at a fix displacement (typically 1.10 mm), then the membrane displaces back, and the  $C$ -reading is taken similarly to the  $A$ -reading. The only difference is that the hole made by the blade may remain stable and the reading may reflect the pore water pressure.

The mechanical details of the DMT are shown in Fig. 3. Behind the membrane there is a sensing disc which is stationary and kept in place by a plastic seating. A non-conductive, quartz cylinder is pushed by a metallic conductive spring-loaded cylinder against the membrane centre. The blade works like an electric switch, which is active (ON) if there is electric contact between the sensing disc and the steel body of the blade or inactive (OFF) if they are electrically isolated.

Once the blade is advanced at the test depth, the horizontal pressure of the soil flattens the membrane against the sensing disc and the contact is active. When the internal pressure counterbalances the external soil pressure, the membrane starts to expand horizontally, (“lift off”) losing electric contact with its support. The contact interruption detects the instant for recording the lift-off pressure, defined as the  $A$ -pressure.

It follows that immediate stress drop, when the effect of dynamic multiplier may not be apparent, is missing in the  $A$ -reading. All the sequential  $A$ -readings are obtained with slight displacement of the soil.

### 1.3 Goal of paper

The aim of the research is to suggest a simple, empirical evaluation mode for the short DMTA dissipation test which can be implemented into the test.

Before taking the  $A$ -reading of DMT, there is a pause period of about 15 s. The MEDUSA DAS has the capability to record the short dissipation data between the stop of the penetration and the  $A$ -reading in every 20 ms.

Due to the DAS system, the excel software was used for the evaluation in the very first stage of the research. Instead of the relaxation equation of the exponential Poynting-Thomson model, a simple power function was fitted on the data.

In this work, this procedure is analysed statistically using some series of short dissipation test records made at the Araquari test site in two soil layers.

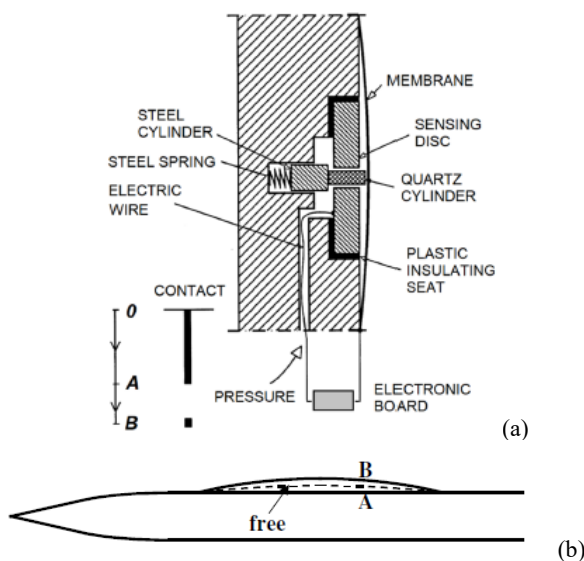


Figure 3.(a) Mechanical details, (b) profile of the non-planar DMT membrane.

## 2. Materials and Methods

### 2.3 The Araquari site and measurements

The project was developed in Brazil, on the coastal plain in the north of the state of Santa Catarina, municipality of Araquari. The profile at the Araquari test site is shown in Fig. 4.

The evolution of the coastal plains of the mentioned states can be divided into eight stages. For the study area, two steps are identified as of greater relevance.

The events that occurred in stage four were the penultimate transgression which happened 120,000 years ago (Upper Pleistocene) when the sea was 8 m above the current level and some sedimentation of fines took place. In step five, the marine sandy terraces of the Pleistocene formed.

The testing program consisted of 3 days. The short dissipation test was made every 20 cm and data were sampled at a frequency of 20 ms. The penetration rate was generally 2 cm/s.

In the first stage of the evaluation of the Araquari project work, out of the Day 1 data (0.2m – 6.60 m) 11 short tests and out of Day 3 data (12.2m – 19.6m), 18 short tests were considered. The Day 2 data (12.2m – 19.6m) have not been evaluated as yet.

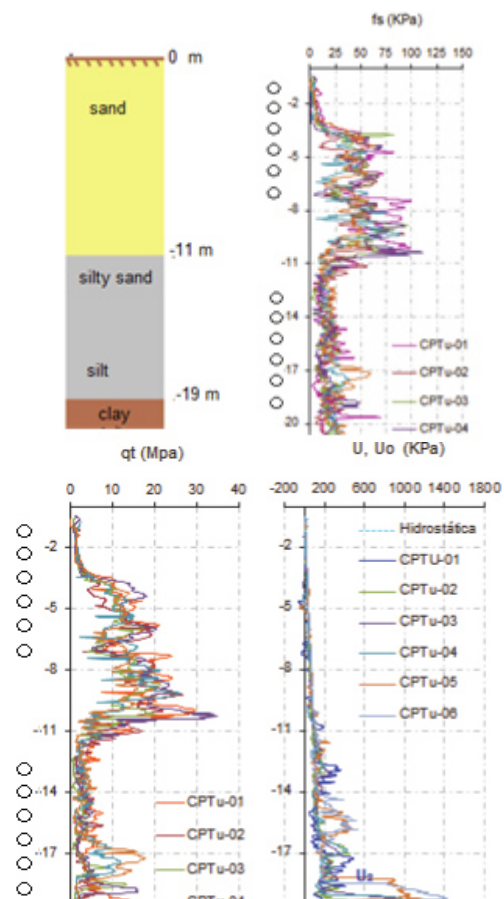


Figure 4. Araquari test site. Soil profile, CPTu  $f_s$  data. CPTu excess pore water pressure,  $u_0$  and CPTu  $q_c$  data.

## 2.2 Evaluation method of short dissipation

The following empirical equation was fitted on the normalised data for the characterization of the short DMT dissipation test records, fitted by the excel graphics program:

$$\sigma(t) = at^b \quad (3)$$

Using the fitted equation, the stress change parameter  $\Delta\sigma$  was computed:

$$\Delta\sigma = \sigma(t_i) - \sigma(t_i + \Delta t); \quad (4)$$

where the  $t_i$  initial time value was the first recorded time value,  $\Delta t = 15$  s was used generally for the final time value.

The excel least-squares fitting process produced a measure – r-squared ( $R^2$ ) – which is 1 minus the ratio of the variance of the residuals to the variance of the dependent variable, expressing what fraction of the variance is explained by the fitted empirical function.

The delta  $\Delta\sigma$  is negative for stress increase ( $\text{sign}(\Delta\sigma)=-1$ ), positive for stress decrease ( $\text{sign}(\Delta\sigma)=1$ ). The exponent  $b$  is positive for stress increase and negative for stress decrease.

The value of  $R^2$  is close to 1 if the noise is small and its value is small if the noise is large. The latter may occur due to “other effects” such as the measuring depth is close to a layer boundary or a permeable layer, or if the DMT-soil contact is changing during the test due to the change in the residual stress state, etc. In other words, the low  $R^2$  may indicate if more than one phenomenon influences the dissipation.

## 3. Results

In every case, 15 s long dissipation period was considered. The empirical Eq (3) was fitted on the measured data. The results are shown in Figs 5 to 8 and Tables 2, 3 separately for the two layers.

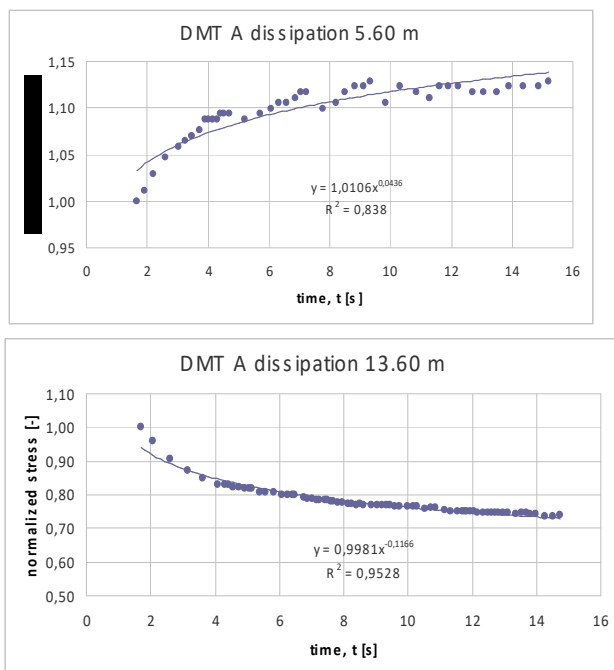


Figure 5. Large  $R^2$  behavior. (a) Sand layer. (b) Silt layer.

The measured dissipation records indicate saw-tooth-like, frictional features, similar to Fig. 1. The size of the steps (saw-teeth) seemed to be dependent on the soil friction angle. Typical measured – fitted curves are shown in Figs. 5 to 7.

The main features of the short dissipation were as follows in case of high  $R^2$ , in saturated sand, the  $A$ -reading was increasing with time, in silt it was decreasing with time.

The model fitting results and the derived parameters are summarized for sands in Table 2, for silts in Table 3, and in Fig. 8.

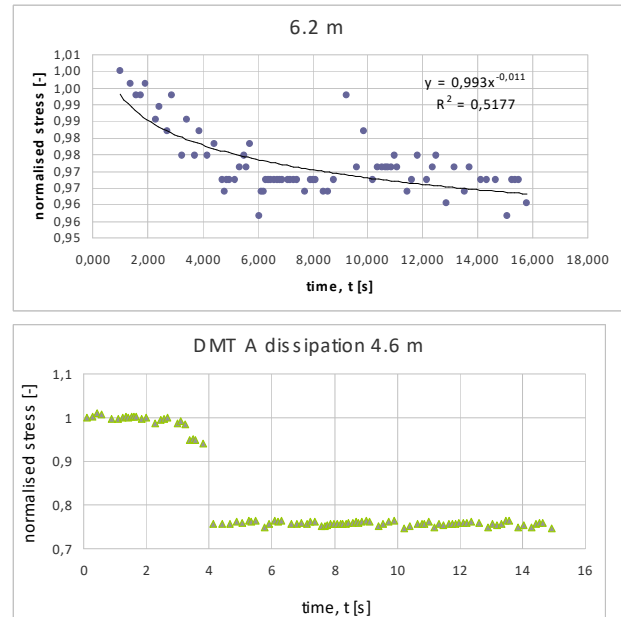


Figure 6. The Araquari test site, sand data, low  $R^2$  sand behavior, with scatter and discontinuity in two depths.

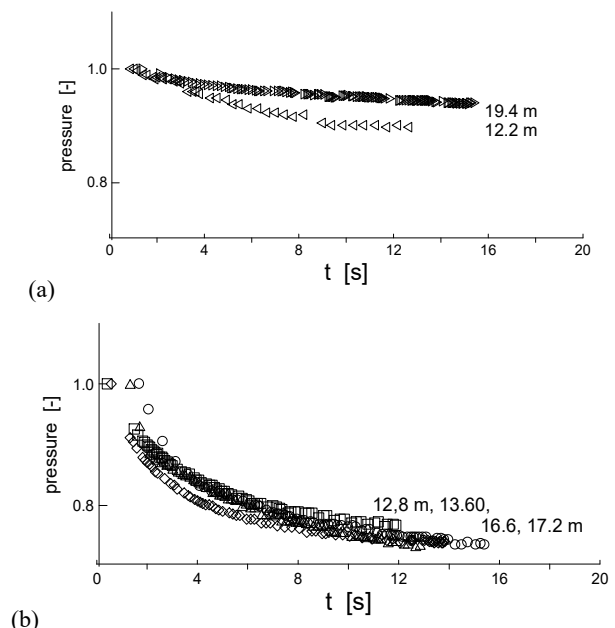


Figure 7. Araquari test site, silt data. Small delta at small  $R^2$  indicating layer boundaries. Large delta at large  $R^2$  indicating large positive excess pore water pressure.

**Table 2.** Day 1 (0.2m – 6.60 m) Sandy soils are indicated by orange (characterized by low  $R^2$  and negative delta)

| Z in m | delta -  | $R^2$ - | exponent - |
|--------|----------|---------|------------|
| 1.20   | 0.097329 | 0.898   | -0.038     |
| 2.20   | 0.081275 | 0.6126  | -0.03      |
| 3.20   | -0.08489 | 0.5975  | 0.0381     |
| 5.00   | 0.02017  | 0.5146  | -0.009     |
| 5.20   | 0.043991 | 0.5203  | 0.018      |
| 5.40   | 0.022918 | 0.3366  | -0.01      |
| 5.60   | -0.10863 | 0.8376  | 0.0436     |
| 5.80   | -0.02175 | 0.3654  | 0.0092     |
| 6.00   | 0.01148  | 0.3814  | -0.005     |
| 6.20   | 0.029144 | 0.5214  | -0.011     |
| 6.40   | -0.00532 | 0.0185  | 0.0023     |

**Table 3.** Day 3 (12.2m – 19.6m) Silty soils indicated by red, the sandy intercalations or layer boundaries by yellow

| Z in m | delta    | $R^2$  | exponent |
|--------|----------|--------|----------|
| 12.2   | 0.132231 | 0.9647 | -0.048   |
| 12.4   | 0.184198 | 0.979  | -0.092   |
| 12.6   | 0.225224 | 0.9984 | -0.125   |
| 12.8   | 0.235673 | 0.9839 | -0.116   |
| 13.    | 0.074132 | 0.9889 | -0.046   |
| 13.2   | 0.049502 | 0.68   | -0.023   |
| 13.8   | 0.024037 | 0.7638 | -0.012   |
| 14.    | -0.13838 | 0.9505 | 0.0657   |
| 15.    | -0.02919 | 0.4695 | 0.0192   |
| 16.    | 0.167442 | 0.8888 | -0.085   |
| 17.    | 0.068381 | 0.8562 | -0.017   |
| 17.2   | 0.255294 | 0.9919 | -0.086   |
| 17.6   | 0.353461 | 0.9987 | -0.172   |
| 17.8   | 0.02097  | 0.2608 | -0.005   |
| 18.    | -0.07679 | 0.7851 | 0.017    |
| 18.6   | 0.055185 | 0.9961 | -0.027   |
| 19.4   | 0.059649 | 0.9895 | -0.026   |
| 19.6   | 0.054675 | 0.9884 | -0.027   |

The main features of the short dissipation in terms of the parameters were as follows.

In saturated sand, the small  $R^2$  indicated very scattered behaviour, rarely even discontinuities (Fig. 6).

In saturated silt high  $R^2$  indicated larger absolute valued delta and larger excess pore water pressure. In saturated silt small  $R^2$  was observed in the vicinity of permeable layers/layer boundaries.

The delta was negative in the sandy parts, positive in the more plastic parts (the reverse was true for the exponent.), on condition that the  $R^2$  was high (i.e. if the homogeneous sand or homogeneous clay behaviour was assessed).

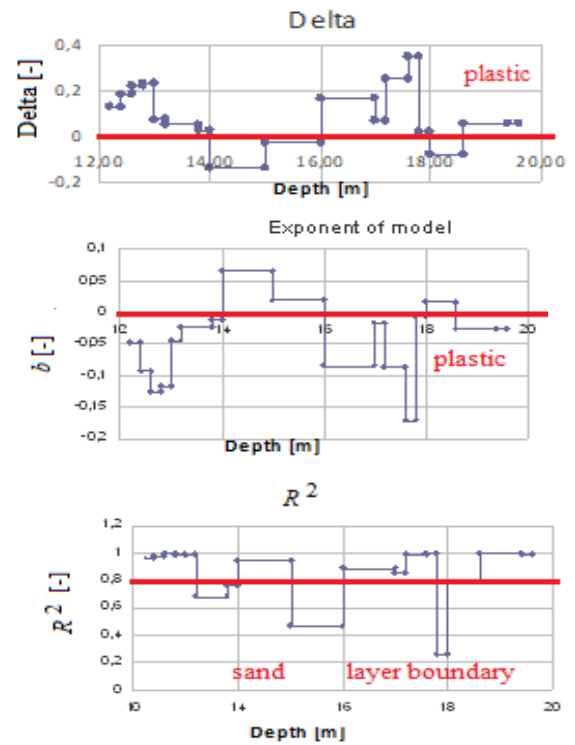


**Figure 8.** (12.2m – 19.6m) Plastic-granular separation, plastic soils have positive delta and negative exponent, granular soils have negative delta, positive exponent and smaller values of  $R^2$ .

In the sand layer, the  $R^2$  was lower than 0.8 in about 80% of the cases indicating that complex phenomena may take place (see Table 2 with colour). In the silt layer, the  $R^2$  was mostly high, the low values (Table 3, Fig. 8, about 20% of the tested cases) may have indicated sand seems and layer boundaries with vertical seepage.

## 4. Discussion

### 4.1 Phenomena

#### 4.1.1 Residual stress state

The CPT is a displacement - type model pile due to the jacking. It is well-known that there are residual stresses during displacement piling, which are small in clay and are significant in sand where huge negative side friction appears above the tip (Appendix). The dissipation may cause to be an increase or a decrease with time, respectively. In accordance with this, the re-driving resistance is less in clays and is larger in sand at the end of the first driving than at the beginning of the first driving and the reverse is true later, in a few days after than at the end of the first driving. Both the theoretical analyses and the construction experiences in relation to re-driving resistance of piles (Yang 1956) indicate a clear distinction between sand and plastic soils.

Therefore, it may be assumed on the basis of the foregoing experiences that plastic and granular soil behaviour separates in the beginning of dissipation in clay or sand due to the residual stress state. This hypothesis is supported by the foregoing statistical evaluations known from literature, showing some additional plasticity dependence.

#### 4.1.2 The vertical equilibrium condition

It is well-known that there is a plastic zone around the displacement piles, where strain localizations may take place, and may be bounded by slip surfaces.

The vertical normal force equilibrium condition of (a part of) the hollow cylindrical soil body around the CPT can be considered (Imre 1988). Since it is bounded by slip surfaces at the outer boundary with assumingly constant soil reaction, the load transferred on the shaft, at inner surface of the cylinder is linked with the vertical soil normal stress at the bottom of the hollow cylinder (shoulder level).

Any change in the load transferred on the shaft may result in a change in the vertical soil normal stress at the bottom of the hollow cylinder (shoulder level).

This link may explain the saw-tooth-like stress variation (the shaft force is frictional) and the qualitatively different features in sand (with scatter and jumps, Fig. 6) and in  $\sim$ NC clay, due to different residual stress state. There are negative residual side friction force in sand the dissipation of it may be causing increasing total normal stress and discontinuous changes at the shoulder level.

#### 4.1.3. Radial stress dissipation

The radial stress release components (irrespective of the effect of residual stress state) are the dynamic-static transition (which appears in case of continuous data acquisition before dissipation which is not the case for the DMTA), consolidation and thixotropic hardening in the failure zone.

The consolidation is needed to be modelled with time dependent constitutive law, the initial condition can be identified except the size of the displacement domain.

The time dependent constitutive law result in total stress relaxation which has the most significant effect at small  $t$ , due to the log law.

The initial condition is permeability and phase transition dependent. In NC clays and in sand the penetration is undrained or drained, respectively.

Moreover, the penetration into saturated sand entails a phase transition from contraction (positive excess pore pressure under the tip) to dilation, resulting in negative excess pore water pressure (see eg., the loosened zone around the shaft, Kouretzis et al. 2014). This fact may explain the presence of high negative residual stress state.

#### 4.2 Similar tests

Both in the S832 CPT local side friction short dissipation test and the DMTA short dissipation test the granular and  $\sim$ NC plastic soils separated since the time dependent change was increase in sand and decrease in NC plastic soils. The only difference was that in DMTA the immediate stress drop was missing since the  $A$ -reading was taken after a slight displacement of the system.

The S832 CPT local side friction and cone resistance short dissipation tests were evaluated by an exponential function, the DMTA dissipation test by a power function. The result was also similar, the parameters indicate the dependence on plasticity and soil type.

It can be noted that the DMTA dissipation test and the PSL dissipation test of CPT are also similar, as first mentioned by Marchetti et al. 1986.

#### 4.3 Short DMTA dissipation at Szeged ELI site

The mean Szeged profile with  $\sim$ NC sands and clays is shown in Fig. 10 (Imre at al. 2022). The DMT dissipation tests made in Szeged test site and in Araquari are similar (Figs. 5-7, 10). In the companion paper these are evaluated.

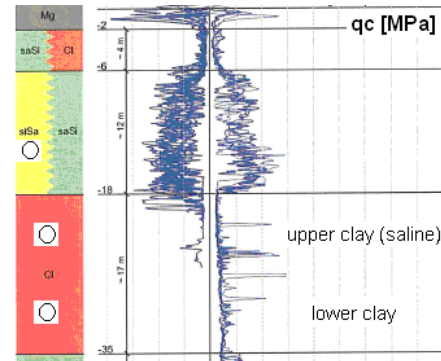


Figure 9. Szeged, ELI, soil profile, with some DMTA dissipation tests indicated

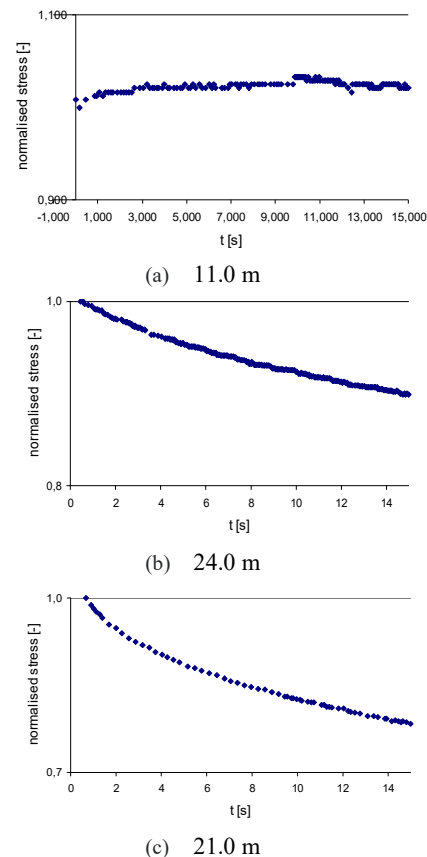


Figure 10. Szeged, ELI, 2020-DMT short dissipation test records (Marchetti, (2020)) (a) sandy soil, (b) more plastic clay and (c) less plastic, saline clay.

### 5. Summary, conclusions

#### 5.1 Statistical analyses, parameters

In this work some DMTA short dissipation test records measured in Araquari test site, Brasil, were characterized by a simple empirical model which can be used to indicate if the dissipation is characterized by one or more phenomena.

A simple power equation was fitted on the measured

data, introduced. 11 and 18 short dissipations records were considered in a sand layer and a silt layer, resp. The parameters of the model were statistically evaluated.

The so determined three model parameters: the stress change ( $\Delta$ ) parameter, the exponent parameter and the  $R^2$  were used for the characterization of the soil related to the short DMT dissipation test records since all model parameters were related to the soil type.

In general, the plastic soils had positive  $\Delta$  and negative exponent, the reverse was true for granular soils as a tendency (the fine sandy soils may have had  $\Delta$  with either small negative or small positive and the exponent was small positive or small negative).

Computing the mean and the Standard Deviation of the parameters of Tables 2 and 3, the results are shown in Tables 4 and 5. The absolute value of the mean of the  $\Delta$  and the exponent was larger by at least one order of magnitude for the silt than for sand.

The  $R^2$  was statistically large in plastic soils and small low in sands. The reason for the difference was that the residual stresses in the equipment (see the Appendix) were negligible in clay and large in sand.

The vertical normal force equilibrium condition of a hollow cylindrical soil body around the CPT in the plastic zone may link the vertical soil normal stress at the level of the shoulder with the load transferred on the shaft.

The dissipation may change the frictional force transferred on the shaft and, therefore, the normal stresses at the shoulder level.

This and the different residual stress state may explain the saw-tooth-like stress variation, and the fact that the short dissipation curves in sand in plastic soil is different.

**Table 4.** Day 1 (0.2m – 6.60 m) Sandy soils; mean, standard deviation and coefficient of variation (Table 2)

|         | $\Delta$ [-] | $R^2$  | exponent [-] |
|---------|--------------|--------|--------------|
| mean    | 0.0078       | 0.5094 | 0.0007       |
| SD      | 0.0623       | 0.2419 | 0.0254       |
| mean/SD | 7.9902       | 0.4749 | 34.0198      |

**Table 5.** Day 3 (12.2m – 19.6m) Silty soils; mean, standard deviation and coefficient of variation (Table 3,  $R^2 > 0.95$ )

|         | $\Delta$ [-] | $R^2$  | exponent [-] |
|---------|--------------|--------|--------------|
| mean    | 0.1630       | 0.9880 | -0.0765      |
| SD      | 0.1040       | 0.0103 | 0.0501       |
| mean/SD | 0.6379       | 0.0104 | -0.6544      |

**Table 6.** Day 3 (12.2m – 19.6m) Silty soils; mean, standard deviation and coefficient of variation (Table 3)

|         | $\Delta$ [-] | $R^2$  | exponent [-] |
|---------|--------------|--------|--------------|
| mean    | 0.0953       | 0.8630 | -0.0447      |
| SD      | 0.1240       | 0.2076 | 0.0585       |
| mean/SD | 1.3010       | 0.2405 | -1.3088      |

The CPT is a displacement - type model pile due to the jacking, which means different residual stress state for sands, NC and OC plastic soils.

In sand, the increasing stress values, scatter and jumps may appear since huge negative residual side friction

force dissipates. In stiff clay small positive, in soft clay near zero residual stress may appear (see the Appendix).

It is well-known that there are residual stresses due to displacement piling, which are small in clay and are significant in sand where huge negative side friction appears above the tip (Appendix). The time dependent stress release cause vertical force redistribution, and a decrease in the absolute value of the negative or positive residual stresses pointwise, along the shaft.

Due to the different residual stress state and the different consolidation parameters, the foregoing parameters may be used for approximate soil identification. The separation of sand and NC plastic soils can be made in this way.

It can be concluded the local side friction and DMTA short dissipation tests can be used to assess the sands and the soft plastic soils, thin sand layers and layer boundaries. All short dissipation tests show plasticity dependent stress variation.

The theoretical analyses on residual stress and the construction experiences in relation to re-driving resistance of piles (Yang, 1956) indicate a clear distinction between sand and soft plastic soils. This explain why soft plastic and granular soil behaviour separate in the beginning of dissipation.

## 5.2 Further research

Further research is suggested on the completion of the data processing, collecting lab test results and longer dissipation test data at the Araquari test site.

Concerning modelling, since a short dissipation test is taking place before the standard *A-reading*, the short dissipation test of a displacement model pile is necessary to be modelled if the standard *A-reading* is analysed. The dynamic loading, the consolidation and the effect of the time dependency of the soil constitutive law (including the effect of creep and relaxation) are to be considered. It can be tested how normal stress state at the shoulder level is influenced by the residual stress dissipation in the whole equipment through the equilibrium condition of the plastic zone.

For the modelling of the short dissipation it is important to be noted that the blade penetration may take place under partly drained and drained conditions, the dissipation test results are not explained solely by the simulations related to the undrained penetration modelling (Kouretzis et al. 2015, Ansari et al. 2015).

## References

- Ansari, Y., Merifield, R., Sheng, D. "A piezocone dissipation test interpretation method for hydraulic conductivity of soft clays", *Soils and Foundations*, 54(6), pp. 1104-1116, 2014.
- Baligh, M. M., Martin, R. T., Azzouz, A. S., Morrisson, M. J. "The piezo-lateral stress cell", In: *Proc. of the 11th ICSMFE San Francisco*, 1985, pp. 841-844.
- Brocheroa, J. L. R., Schnaid, F. "Geotechnical characterization of the Araquari testing site in sand", *Geotecnia*, 148, pp. 55-67, 2020, <http://doi.org/10.24849/j.geot.2020>.
- Imre, E. "Statistical evaluation of simple rheological CPT data", In: *Proc. of XI. ECSMFE*, 1995, pp. 155-161.
- Imre, E. "Skin bearing capacity of piles", In: *Proc. 1st Int. Geotech. Seminar on Deep Foundations on Bored and Auger Piles*, 1988, pp. 421-429.

Imre, E., Rózsa, P., Bates, L., Fityus S. "Evaluation of monotonic and non-monotonic dissipation test results", COGE, 37, pp. 885-904, 2010.

Imre, E., Bates, L., Fityus, S., Hegedus, M., Hortobágyi, Zs., Singh V. P. "Evaluation of dilatometer dissipation test data", In: ISC6, Budapest, 2021-2022. <https://doi.org/10.53243/ISC2020-273>

Imre, E., Bates, L., Fityus, S., Hegedús, M., Singh, V. P. "Coupled models for stress dissipation tests", In: ISC6, Budapest, 2021-2022. <https://doi.org/10.53243/ISC2020-269>

Imre, E., Hegedús, M., Marchetti, D., Juhász, M., Hortobágyi, Zs, Bishop, D., Bates, L. "Comparing dissipation tests of CPTu and DMT", In: 20th ICSMGE Sydney. Australian Geomechanics Society, 2022, pp. 417-422.

Imre, E., Marchetti, D., Juhász, M., Bates, L., Fityus, S. "Least-Squares evaluation of DMT dissipation test data – some preliminary results", submitted IS-Porto 2023.

Kouretzis, G. P., Sheng, D., Wang, D. "Numerical simulation of cone penetration testing using a new critical state constitutive model for sand", *Comput. Geotech*, 56, pp. 50–60, 2014.

Kouretzis, G. P. Ansari, Y. Pineda, J., Kelly, R. Sheng, D. "Numerical evaluation of clay disturbance during blade penetration in the flat dilatometer test", *Géotechnique Letters*, 5, pp. 91–95, 2015. <http://dx.doi.org/10.1680/jgele.15.00026>

Marchetti, S. Totani, G., Campanella, R. G., Robertson, P. K., Taddei, B. "The DMT- $\sigma_{hc}$  method for piles driven in clay", In: Proceedings of In Situ '86. GT. Div. ASCE, June 23-23, Blacksburg, VA, 1986, pp. 765-779.

Monaco, P.(coordinator) "Standardization of Medusa DMT testing" Medusa dilatometer test Pre-standard Reference Test Procedure & Guidelines Report of UnivAQ – DICEAA. Working Group University of L'Aquila, Italy. Version 1.1 – 1st March 2021.

Marchetti, D. "Medusa DMT tests in Szeged", ELI Expertise. 2020.

Poulos, H. G. "Analysis of residual stress effects in piles", *J. Geotech. Engrg ASCE*, 113, pp. 216-22, 1987.

Randolph, M. F., Wroth, C. P. "An analytical solution for the consolidation around displacement piles", *I. J. for Num. Anal. Meth. in Geomechanics*, 3, pp. 217-229, 1979.

Totani, G., Clabrese, M. Monaco, P. "In situ determination of  $\sigma_{hc}$  by flat plate dilatometer", In: Proceedings of ISC-1, Atlanta, Georgia, 1998, pp. 883–888.

Vesic, A. S. "On the significance of residual loads for load response of piles", In: Proc. 9th Int. Conf. Soil Mechs. Found. Eng., Vol. 3 , Tokyo , Japan , 1977, pp. 374 - 379.

Yang, N.-C. "Redriving characteristics of piles". *ASCE Jl. of Soil Mech. and Found. Div.* 1956.

## Appendix

The existence of residual stresses in driven piles after they have been installed has been recognized for some time (Vesic 1977). The analysis of Poulos clarified a very different behaviour of clay and sand (Poulos 1987). The following observations are made (Fig. 11):

1. For the stiff clay, the residual stress near the pile head reaches the limiting tensile shaft resistance, but decreases with depth and changes sign about halfway along the pile.
2. For the soft clay, the residual stresses are small and generally well below the limiting shaft resistance values.
3. For the sand, the residual stresses are substantial and the pile shaft is in a state of tensile slip along most of its length.

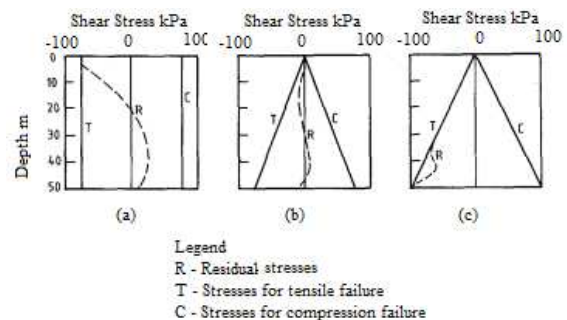


**Figure 11.** Residual shear stresses (a) stiff clay (b) soft clay (c) sand (after Poulos 1987).